

Mouse Anatomical Cardinal Planes and Axes Towards Augmentation for Behavior Analysis

Salvador Blanco Negrete*, Ravi Prakash Joshi*, Rollyn Labuguen*, Jumpei Matsumoto†, Tomohiro Shibata*

*Graduate School of Life Science and Systems Engineering, Kyushu Institute of Technology, Kitakyushu, Japan

†System Emotional Science, University of Toyama, Toyama, Japan

Email: {negrete.blanco771, joshi.ravi-prakash869} @mail.kyutech.jp, labuguen-rollyn@edu.brain.kyutech.ac.jp, jm@med.u-toyama.ac.jp, tom@brain.kyutech.ac.jp

Abstract— In this paper, we propose a visualization framework for mouse anatomical cardinal planes and axes by extending an open-source platform called "3DTracker-FAB" and demonstrate its capability towards augmentation. Previously, the 3DTracker-FAB was only able to determine the mouse anatomical model, showing its head, neck, trunk, hip, and nose. We enhance the software to include body axes and planes of the subject in relation to its anatomical model. This work will help scientist working with animals since anatomical axis and planes are used for describing motion, and anatomical location.

Keywords— Anatomical axis; cardinal planes; mouse behavior analysis.

I. INTRODUCTION

Markerless motion capture systems for living animals and humans have become a very useful tool for behavior analysis and healthcare applications. This type of system provides non-invasive tests on the subjects maintaining lesser effect on the animals natural and social behavior. With the availability of high-resolution cameras and low-cost depth sensing devices, markerless systems have been developing and gaining direction towards automation and augmentation. Experiments where the aim is to understand behavioral activities of the animal, usually involve precise subject's information such as body orientation and its locomotion, which can be inferred from the anatomical planes and axes. Markerless camera systems have recently been integrated into these types of modeling tests for animals such as monkeys and rats [1][2][8]. There are several environments - in a home cage or box or in the wild, where behavioral observations are conducted and measured. Instead of subjective observation, most of these experiments are better evaluated objectively by using computer-assisted tools and computer-generated models. In addition, locomotor assessment is also best described in 3D rather than 2D alone. Hence, animal models have been introduced to represent output analysis on a three-dimensional markerless motion capture system. In this way, researchers and neuroscientists will be able to gather more objective information in a lesser amount of time with the help of computational models [3][5].

Animal behavior analysis are frequently treated and conducted in a controlled environment while securing that the natural behavior of the animals is initially undisturbed. In order to capture and evaluate the subjects' behavioral changes, systems without optical markers are more preferred than the marker-

based systems, which are hard to set-up and quite expensive. Marker-based systems to analyze animal behaviors often induce acrophobia or change in the naturalistic behavior of the subject. Such systems are not suitable to discover and study the differences of motor activity and stress-related actions exhibited by the subjects, most especially for rats and mice, whose movements are very fast. One example of the tests done to understand the behavioral changes on rodents is the open-field test, wherein the subjects are observed on freely moving state. This kind of test is a necessary procedure on genetic and neuroscience research. Recent studies have proposed to integrate 3D mice tracking approaches to the open-field test in order to capture locomotion of not only individual subject [7] but also for social interaction [6]. The works of Unger [9] and Wiltschko [10] emphasize that 3D visualization helps as a tool to quantify objectively rodent behavior with the leverage of generative models and algorithms for tracking.

Although there exist several systems that aim to track and evaluate the movements and social behaviors of the mouse as in [3][4][7], in the best of our knowledge there is no system that has the capability to visualize the cardinal planes and axis. The anatomical planes are the basis for dividing the anatomical subject into symmetrical parts. Any movement parallel to each plane describes a specific oriented motion either in the front, back, side, top, and bottom movements. The effect of individual joint motions will occur not only in one plane but all in three anatomical planes. Hence, it is essential to check on and visualize the cardinal planes. For instance, during standing, the upper limb movements cause changes in the rotation along the transverse plane, flexion/extension on sagittal, and limb raising along the frontal view.

II. METHODOLOGY

Our work proposes the extension on a recently opened and publicly available rodent tracking software called 3DTracker-FAB [12]. Section A discusses the capabilities of the open-source platform that we built upon. Section B presents the assumptions and descriptions of the anatomical cardinal planes being included to the previous system.

A. 3DTracker-FAB

3DTracker-FAB employs multiple depth cameras to observe the animals in a square-field box arena. A sample dataset is

accessible on the 3DTracker-FAB webpage, which contains three-dimensional point cloud information for a 170-second male rodent's interaction. The 3D video was recorded from four different Intel RealSense Camera R200 depth sensors, situated in each face of the box. Each frame represents three-dimensional point cloud data, where the model will be fitted upon. The fitting scheme is based on simulating movements of physical entities such as spheres constrained by several types of forces.

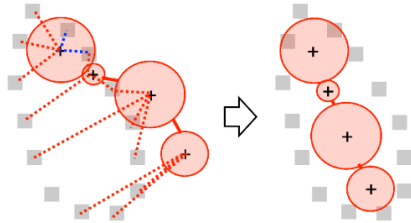


Figure 1. Concept of the position estimation algorithm. The position of body parts is denoted with the cross mark. The hull of the mouse is represented by the gray squares. The mouse skeleton is denoted in red. Left: before fitting. Right: after coverage. Adapted with permission from "A 3D-Video-Based Computerized Analysis of Social and Sexual Interactions in Rats," p. 4. [3]. doi:10.1371/journal.pone.0078460.g002

The spheres representing body features move in accordance to the hull-base getting algorithms formulated in (1) and (2). Several types of forces are acting on the body model of the mouse. Attraction force evokes the model into the hull points and repulsive force retains the model inside the hull so that the model will not get away from the 3D points. These vectors forces applied to each body part B are implemented using the following equations of f_a and f_r respectively.

$$\vec{f}_a = \alpha \sum_l^n \overrightarrow{BP_l} \quad (1)$$

$$\vec{f}_r = \beta \sum_j^m \overrightarrow{Q_jB} / |\overrightarrow{Q_jB}| \quad (2)$$

where α and β are constants, $P_l (l = 1, \dots, n)$ and $Q_j (j = 1, \dots, m)$ are regions of points that make the 3D hull.

Each frame in the video shows the fused point cloud from the views of four depth sensors. The spherical models are fitted to the point clouds of the mice using the concept described in Figure 1. The final output of the 3D Tracker-FAB fitting model is in Figure 2.

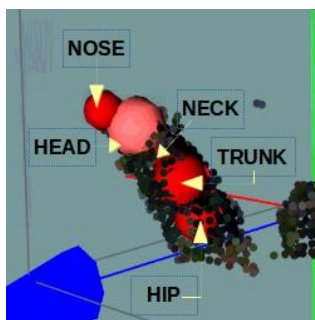


Figure 2. 3D Tracker-FAB original model. The red spheres represent the body parts. The black-gray points represent the point cloud.

The 3DTracker-FAB, only extracts the head, neck, trunk, hip, and nose features to create the anatomical model of the mouse as shown in Figure 2. It is insufficient to describe the orientation

nor the specific sections of the full body of the mouse. In order to extract and estimate the location of anatomical axis and planes, we take into account the relative positions from the given features of 3DTracker-FAB. We only analyze the frames where the straightened body of the mouse is fully visible. These are the set of frames when the mouse stands. Two researchers have evaluation whether the planes are depicted correctly or not.

B. Anatomical Axis and Planes

Our method assumes that the spheres of the nose, head, body, and hip features coming from the 3DTracker-FAB are aligned to each other. In addition, the y coordinates of x_1 and x_2 vertices for creation of the sagittal plane and frontal plane are manually set 10% higher than the nose height, NP . The y coordinates of x_3 and x_4 vertices of the same planes are defined as the ground position i.e., zero. The cardinal plane locations also depend on the axes computation as explained further.

1) Anatomical Axis

Anatomical axes are imaginary axes utilized as a reference to the structures of animals. Hyman [11] defines anatomical axis as:

- The sagittal axis corresponds to a line that goes from the dorsal to ventral surfaces and that is in the sagittal plane.
- The longitudinal axis corresponds to a line that goes from head to tail and that is in the sagittal plane.
- The transverse axis corresponds to a line in the transverse plane going from side to side.

a) Sagittal axis

The sagittal axis vector v_{SA} is calculated as the vector that goes through the trunk point ($P3$), and that is perpendicular and goes through the line defined by the hip ($P2$) and head ($P1$). In Fig 3 the point of intersection of the vector v_{SA} with the line $P2 - P1$ is marked as $P4$.

$$v_{21} = P2 - P1 \quad (3)$$

$$v_{31} = P3 - P1 \quad (4)$$

$$v_{SA} = [(v_{31} \cdot v_{21}) / |v_{21}|^2] \cdot v_{21} - v_{31} \quad (5)$$

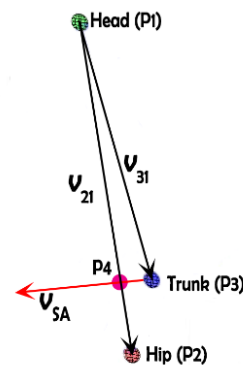


Figure 3. The sagittal axis v_{SA} , in the context of the body features, is computed using equations (3)(4)(5).

b) *Longitudinal axis*

The longitudinal axis vector v_{LA} is calculated as the vector perpendicular to the transverse axis vector v_{TA} (equation 7) and the sagittal axis vector v_{SA} .

$$v_{LA} = v_{TA} \times v_{SA} \quad (6)$$

c) *Transverse axis*

The transverse axis vector v_{TA} is calculated as the vector perpendicular to the line defined by the Hip-Head (v_{21}) and the Trunk-Hip (v_{31}) vectors.

$$v_{TA} = v_{21} \times v_{31} \quad (7)$$

2) *Anatomical Planes*

The anatomical planes are also utilized as a reference to the structures of animals which are typically symmetrical [11].

Hyman [11] defines anatomical planes as:

- Sagittal plane is any vertical longitudinal plane through the body.
- The frontal plane is any horizontal longitudinal section through the body.
- The transverse plane cuts vertically across the body at right angles to the sagittal and horizontal planes.

In this paper, each of the three anatomical planes is described by their vertices $x = [x_1 x_2 x_3 x_4]'$. The location in the 3D space of the vertices is obtained as a linear combination of two anatomical axis vectors v_{AA1} and v_{AA2} and a starting point SP.

$$\begin{bmatrix} x_1 \\ x_2 \\ x_3 \\ x_4 \end{bmatrix} = \begin{bmatrix} a_1 * v_{AA1} + b_1 * v_{AA2} + SP \\ a_2 * v_{AA1} + b_2 * v_{AA2} + SP \\ a_3 * v_{AA1} + b_3 * v_{AA2} + SP \\ a_4 * v_{AA1} + b_4 * v_{AA2} + SP \end{bmatrix} \quad (8)$$

Equation 8 describes the general equation for the anatomical planes. As an example, in the sagittal plane (Figure 4) the v_{AA1} and v_{AA2} correspond to the longitudinal axis vector v_{LA} and the sagittal axis vector v_{SA} respectively. The a_{1-4} and b_{1-4} coefficients values are calculated using (8), the aforementioned assumptions and taking into account the orientation of the planes with respect to the body of the mouse.

a) *Sagittal plane*

We estimate the sagittal plane as a linear combination of the longitudinal axis v_{LA} and the sagittal axis v_{SA} .

$$x = a * v_{LA} + b * v_{SA} + SP \quad (9)$$

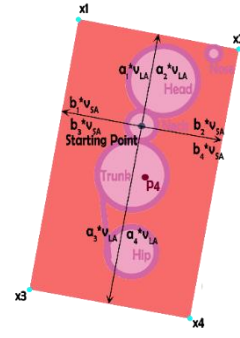


Figure 4. Sagittal plane, side view. In the sagittal plane the longitudinal axis vector v_{LA} corresponds to v_{AA1} (equation 8), in the same way v_{SA} corresponds to v_{AA2} . Note that for expository proposes the vectors are drawn from the starting point (SP), also note that in the sagittal plane $a_1 * v_{LA} = a_2 * v_{LA}$, $a_3 * v_{LA} = a_4 * v_{LA}$, $b_1 * v_{SA} = b_3 * v_{SA}$, and $b_2 * v_{SA} = b_4 * v_{SA}$. As an example, the vertex $x_1 = a_1 * v_{LA} + b_1 * v_{SA} + SP$ (equation 8). Adapted with permission from "A 3D-Video-Based Computerized Analysis of Social and Sexual Interactions in Rats," p. 4. [3].
doi:10.1371/journal.pone.0078460.g002

The equations (10) and (11) for the coefficients a and b are derived from equation (8) when the constraints are set as explained in Section B. NP_y is the y component of the nose point, SP_y is the y component of the starting point, v_{SAy} the y component of the sagittal axis vector, and v_{LAy} the y component of the longitudinal axis vector.

$$a = \begin{bmatrix} (NP_y * 1.1 - SP_y - v_{SAy})/v_{LAy} \\ (NP_y * 1.1 - SP_y + v_{SAy})/v_{LAy} \\ (-SP_y + v_{SAy})/(v_{LAy}) \\ (-SP_y - v_{SAy})/(v_{LAy}) \end{bmatrix} \quad (10)$$

$$b = \begin{bmatrix} -1 \\ 1 \\ -1 \\ 1 \end{bmatrix} \quad (11)$$

b) *Frontal plane*

We estimate the frontal plane as a linear combination of the longitudinal axis v_{LA} and the frontal axis v_{FA} .

$$x = a * v_{LA} + b * v_{FA} + SP \quad (12)$$

$$a = \begin{bmatrix} 1 \\ 1 \\ -1 \\ -1 \end{bmatrix} \quad b = \begin{bmatrix} -1 \\ 1 \\ -1 \\ 1 \end{bmatrix} \quad (13)$$

c) *Transverse plane*

The transverse plane is calculated as a linear combination of the sagittal axis v_{SA} and the transverse axis v_{TA} .

$$x = a * v_{SA} + b * v_{TA} + SP \quad (14)$$

Equations for a and b are the same as in (10) and (11).

III. RESULTS AND DISCUSSION

We determine the performance of the visualization when the mouse is in standing state. Figure 5 shows the tri-anatomical axes (sagittal, longitudinal and transverse axis) superimposed on the subject's body. Using the corresponding RGB images of these frames from two views, the axes on the 3D data gives more affirmation to which direction the mouse is inclined. The sagittal axis identifies where the mouse is facing in the point cloud dataset.

Moreover, Figure 6 shows the anatomical body planes – frontal, transverse and sagittal plane. Each plane cut the subject into halves to pertain divisions of symmetry of the body. The planes also move along the anatomical axes that are visualized in the beginning. These cardinal planes were made visible to attempt for describing the 3D motions of the mouse without using markers. For instance, the movement of rearing or standing is visualized as a motion occurring with all three planes. The most observable movement would happen on the hip that is expressed on the sagittal plane, changes in the left and right sides of the mouse. Likewise, the frontal and transverse planes are affected. The hip exhibits extension and flexion on the sagittal plane and at the same time, emphasizing rotations on the bottom part of the mouse and the movements in front, to complete a standing motion.

All the anatomical planes and axes are simultaneously depicted in Figure 7.

A. Anatomical Axis

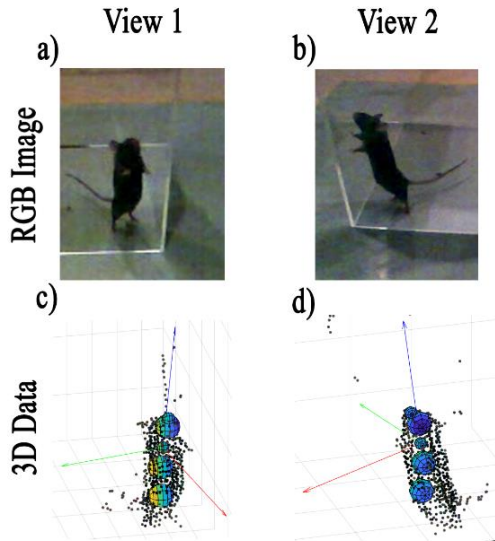


Figure 5. Anatomical axes - sagittal axis (red), longitudinal axis (blue), and transverse axis (green) with their corresponding RGB images.

B. Anatomical Planes

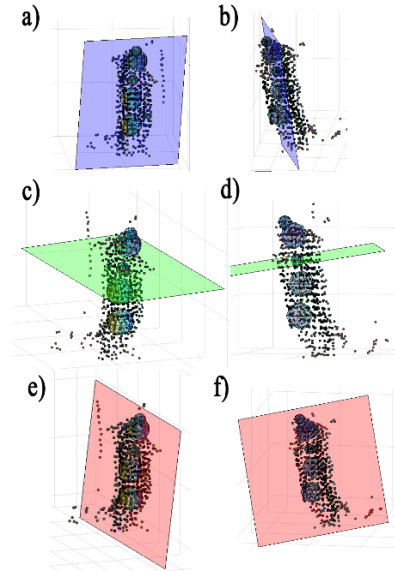


Figure 6. The three different body planes shown separated with the mouse in a standing position: a) b) Frontal plane (blue). c) d) Transverse plane (green). e) f) Sagittal plane (red). The views are the same as in Figure 5.

C. Final result

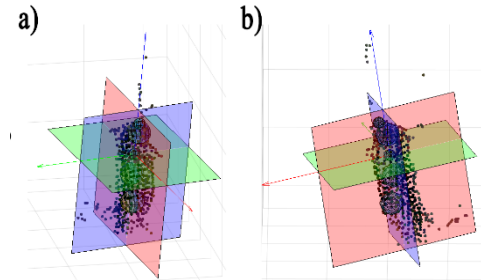


Figure 7. Body axes & planes displayed simultaneously: sagittal plane (red), frontal plane (blue), transverse plane (green), sagittal axis (red), longitudinal axis (blue), and transverse axis (green). The views are the same as in Figure 5.

D. Empirical Evaluation

Sequence of nine consecutive frames during the mouse stands is evaluated by two researchers. As shown in Table 1, the success rate of plane extraction is determined through observation, whether the planes matched the researchers' expectation. For instance, two of the sagittal planes did not pass the criterion since these planes are slanted which do not divide the mouse into left and right side symmetrically.

	Transverse Plane	Sagittal Plane	Frontal Plane
Success Rate	9/9	7/9	4/9

Table 1. Evaluation of consecutive frames with the mouse in a standing position. The transverse plane, frontal plane, and sagittal plane were evaluated.

Overall, the system is capable of displaying the different axial planes, and giving reference to the viewer of the position, location of body parts and structures of the mouse, even in the failure case. The failure in the frontal plane corresponds to a slight misalignment as shown in Figure 8 a) b), the failure in transverse plane is caused by the mouse being in transition to a full standing position i.e. the mouse is in a curved posture as shown in Figure 8 c).

E. Expected Failure Case

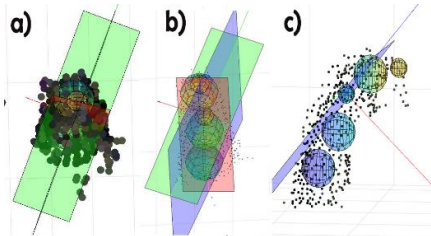


Figure 8. Expected failure case. The mouse from a top front view a) Failure case highlighting the point cloud information. b) Failure case highlighting the body features as provided by the 3D tracker. c) Error in the frontal plane caused by the mouse being in a curved posture.

As expected when the spheres representing body features provided by the 3DTracker-FAB are not correctly aligned, the anatomical axis and plane axis are misaligned. In the worst case, the planes may be switched. Figure 8 a) b) demonstrates when the trunk feature was aligned to the right, which causes all the planes to shift to the left. When the mouse is in a curved posture there is an error in the placement of the frontal plane as shown in c).

IV. CONCLUSIONS

Our application has integrated a new capability to infer the anatomical axis and plane locations of the mouse. Objective analysis will be quicker through this assistive tool for neuroscientists. We have extended the approach on hull fitting to extract the body phase representations of the mice at a frame rate of 4-5 fps. The planar visualization has also been envisioned for mapping onto 2D videos to provide additional information and augmentation on the mouse's body. Including the set of anatomical axes and planes into the three-dimensional spherical model has enriched the description for the mouse's anatomical motion.

ACKNOWLEDGMENT

This work was supported by the Grant-in-Aid for Scientific Research from Japan Society for the Promotion of Science (No. 16H06534).

REFERENCES

- [1] J. D. Foster, P. Nuyujukian, O. Freifeld, H. Gao, R. Walker, S. I. Ryu, T. H. Meng, B. Murmann, M. J. Black, and K. V. Shenoy. A freely-moving monkey treadmill model. *Journal of neural engineering*, 11(4):046020, 2014.
- [2] J. Matsumoto, H. Nishimaru, T. Ono, and H. Nishijo. 3d-video-based computerized behavioral analysis for in vivo neuropharmacology and neurophysiology in rodents. In *In Vivo Neuropharmacology and Neurophysiology*, pages 89–105. Springer, 2017.
- [3] J. Matsumoto, S. Urakawa, Y. Takamura, R. Malcher-Lopes, E. Hori, C. Tomaz, T. Ono, and H. Nishijo. A 3d-video-based computerized analysis of social and sexual interactions in rats. *PLOS ONE*, 8(10):1–14, 10 2013.
- [4] A. Nakamura, H. Funaya, N. Uezono, K. Nakashima, Y. Ishida, T. Suzuki, S. Wakana, and T. Shibata. Low-cost three-dimensional gait analysis system for mice with an infrared depth sensor. *Neuroscience research*, 100:55–62, 2015.
- [5] T. Nakamura, J. Matsumoto, H. Nishimaru, R. V. Bretas, Y. Takamura, E. Hori, T. Ono, and H. Nishijo. A markerless 3d computerized motion capture system incorporating a skeleton model for monkeys. *PLoS one*, 11(11):e0166154, 2016.
- [6] W. S. Redfern, K. Tse, C. Grant, A. Keerie, D. J. Simpson, J. C. Pedersen, V. Rimmer, L. Leslie, S. K. Klein, N. A. Karp, et al. Automated recording of home cage activity and temperature of individual rats housed in social groups: The rodent big brother project. *PLoS one*, 12(9):e0181068, 2017.
- [7] W. I. Sellers and E. Hirasaki. Markerless 3d motion capture for animal locomotion studies. *Biology open*, 3(7):656–668, 2014.
- [8] A. L. Sheets, P.-L. Lai, L. C. Fisher, and D. M. Basso. Quantitative evaluation of 3d mouse behaviors and motor function in the open-field after spinal cord injury using markerless motion tracking. *PLOS ONE*, 8(9):1–13, 09 2013.
- [9] J. Unger, M. Mansour, M. Kopaczka, N. Gronloh, M. Spehr, and D. Merhof. An unsupervised learning approach for tracking mice in an enclosed area. *BMC bioinformatics*, 18(1):272, 2017.
- [10] A. B. Wiltschko, M. J. Johnson, G. Iurilli, R. E. Peterson, J. M. Katon, S. L. Pashkovski, V. E. Abaira, R. P. Adams, and S. R. Datta. Mapping sub-second structure in mouse behavior. *Neuron*, 88(6):1121–1135, 2015.
- [11] L. H. Hyman. *A laboratory manual for comparative vertebrate anatomy*. University of Chicago, p.1. Available at: <https://archive.org/details/cu31924021952902> [Accessed: March 30, 2018].
- [12] J. Matsumoto. 3DTracker-FAB GitHub repository, <https://github.com/ThreeD-Tracker-FAB/3DTrackerFAB-main>, [Online; accessed (March 30, 2018)].